PERGAMON

International Journal of Solids and Structures 37 (2000) 2473–2487

INTERNATIONAL JOURNAL OF SOLIDS and STRUCTURES

www.elsevier.com/locate/ijsolstr

Fracture analysis of cracked orthotropic skin panels with riveted stiffeners

J.R. Yeh*, M. Kulak

Aluminum Company of America, Alcoa Technical Center, Alcoa Center, PA 15069, USA

Received 5 October 1998; in revised form 11 December 1998

Abstract

The stress intensity factors and energy release rates are determined for cracked orthotropic sheets with riveted stiffeners. A closed form solution is used and the approach adopted is based on compatibility of displacements among the sheet, fasteners and stiffeners. Effects of the nonlinear shear deformation of the fasteners, the plastic deformation of the stiffeners, and stiffener cutouts in frames are included in the analysis. A one-bay crack and a two-bay crack with center stiffener either intact or broken are evaluated. The results obtained from the analytical method are compared with finite element results. Good agreement of these results demonstrates the validity and accuracy of the analytical method. © 2000 Elsevier Science Ltd. All rights reserved.

Keywords: Fracture; Analysis; Stiffened panels; Cracked panels; Orthotropic; Riveted stiffeners

1. Introduction

Stiffener-reinforced sheet structures are widely used in aircraft designs based on fail-safe and damage tolerant requirements. A considerable amount of research on crack tip stress intensity analysis has been conducted by many researchers (Romualdi et al., 1957; Poe, 1973; Swift, 1984; Nishimura, 1991). In their papers, the effects of a cracked sheet attached with multiple intact stiffeners and broken stiffeners, the bending flexibilities of sheet and stiffeners, the nonlinear shear deformation of fasteners, and cracked stiffeners have been studied. These results are obtained under a condition that the sheet has isotropic material properties.

Laminated aluminum materials and laminated composites are often orthotropic if regarded as a homogeneous media. Several studies have been conducted for fracture mechanics of laminated orthotropic skin sheets (Yeh, 1988, 1993, 1995). A closed form solution was developed to determine the

* Corresponding author.

PII: S0020-7683(99)00005-0

stress intensity factor and energy release rates for cracked orthotropic sheets with riveted stiffeners (Yeh, 1993). The analysis was conducted within the limitations of elasticity theory.

For low-load, high-cycle fatigue, the analytical method presented by Yeh (1993) can be used to predict the fatigue crack growth of a cracked stiffened panel, and consequently determine the required inspection intervals according to damage tolerant design method. However, for determination of residual strength, the force in the first fastener adjacent to the skin crack is very large when the skin crack crosses the intact stiffener. Therefore, the effects of the nonlinear shear deformation of the fasteners and the plastic deformation of the stiffeners need to be included in the residual strength analysis. In this study, the computer program developed by Yeh (1993) for the elastic analysis is extensively modified to include these two nonlinear effects. The program is also modified to allow for variable cross-section stiffeners simulating the stiffener cutouts in frames.

In the next section, a closed form solution of cracked orthotropic sheets with riveted stiffeners is presented for the displacement compatibility analysis (Swift, 1984). An approach to handle nonlinear effects of fasteners and stiffeners is presented. In Section 3, fracture mechanics parameters, stress intensity factor and energy release rate, are determined for the cracked orthotropic sheets as functions of the applied stress and the corresponding fastener forces. Finally, numerical examples for an orthotropic laminate with one-bay and two-bay cracks are studied and discussed. The accuracy of the present method is demonstrated by comparing the analytical solution with finite element results.

2. Formulation of problem

The analysis model shown in Fig. 1 is a cracked sheet reinforced with riveted stiffeners subjected to a remote uniaxial stress. The crack in the sheet is perpendicular to the loading direction. The number and location of stiffeners and fasteners are arbitrary and not restricted. The sheet is assumed to be orthotropic, with principal directions of orthotropy being oriented parallel to and normal to the crack.

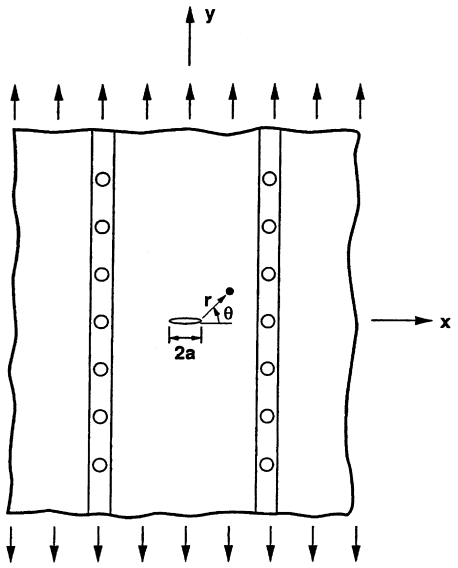

Fig. 1. Schematic of a cracked sheet with riveted stiffeners.

The thickness of the sheet is so small compared with the in-plane dimensions that the problem may be treated as a plane stress problem.

There are two popular ways to determine the fracture mechanics parameters at the crack tip. One is the direct finite element analysis, which can be used to obtain the crack tip stress intensity factor and energy release rate for those complex structures with orthotropic material properties. This analysis requires a considerable amount of computer running time. Another is the displacement compatibility method commonly used for parametric studies in design calculations (Swift, 1984). The latter approach is adopted in this study.

By using the solution of a single crack in an infinite sheet and the principle of superposition, the condition of equilibrium of force and the condition of compatibility of displacements among the sheet, fasteners and stiffeners are formulated. For simplicity, the method of analysis for a single attached stiffener problem is described below.

2.1. Skin displacements

Displacements in the cracked sheet are determined by superposition of the four cases shown in Fig. 2(a–d). Displacements resulting from these four cases are: (1) v_1, the displacement in the uncracked sheet caused by an applied uniform stress, σ_0, (2) v_2, the displacement in the cracked sheet resulting from the stress σ_0 applied to the crack surface, (3) v_3, the displacement in the uncracked sheet due to a fastener force, F, (4) v_4, the displacement in the cracked sheet resulting from the stress (caused by the fastener force F) applied to the crack face.

The displacement v_1 in an uncracked sheet subjected to the remote uniaxial stress, σ_0, shown in Fig. 2(a), is given by:

$$v_1 = \sigma_0 / E_y y \tag{1}$$

where E_y is Young's modulus of the orthotropic sheet in y-direction shown in Fig. 1. In order to

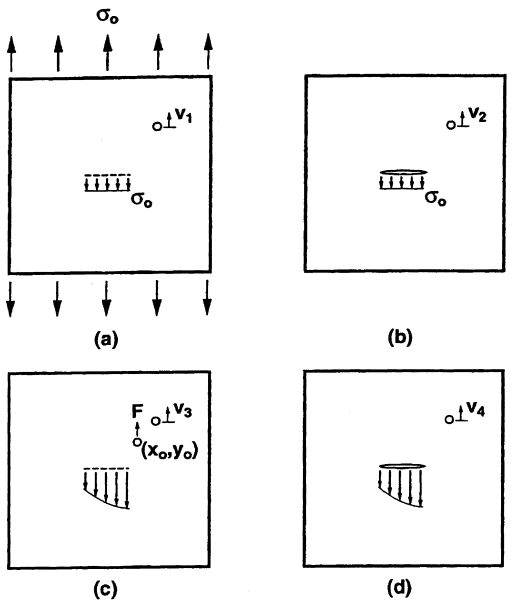

Fig. 2. Displacements that are superimposed to determine total sheet displacement.

determine the other displacements, v_2, v_3 and v_4, the complex stress function approach of Lekhnitskii (1968) is used. For plane stress, the y-component of sheet displacement, v, can be given using two complex stress functions, ϕ and ψ, as:

$$v(x, y) = 2Re\left[q_1\phi(z_1) + q_2\psi(z_2)\right] \tag{2}$$

where Re represents the real part of the complex function, and

$$z_m = x + s_m y, \tag{3}$$

$$q_m = \frac{1 - \nu_y s_m^2}{s_m E_y} \quad (m = 1, 2) \tag{4}$$

with s_m being the roots of the characteristic equation

$$s^4 + \left(\frac{E_x}{G_{xy}} - 2\nu_x\right)s^2 + \frac{E_x}{E_y} = 0 \tag{5}$$

in which E_x, E_y, G_{xy}, ν_x and ν_y are the elastic constants of the orthotropic sheet and $\nu_x/E_x = \nu_y/E_y$. Note that the imaginary part of s_m is larger than zero, since the above characteristic equation cannot have real roots for any ideal elastic body (Lekhnitskii, 1968).

The displacement v_2 in the cracked sheet subjected to an uniform applied stress σ_0 on the crack surface may be obtained from the following two complex stress functions (Sih and Liebowitz, 1968)

$$\phi_2(z_1) = \frac{s_2}{s_2 - s_1}\frac{\sigma_0}{2}\left(\sqrt{z_1^2 - a^2} - z_1\right) \tag{6a}$$

$$\psi_2(z_2) = \frac{s_1}{s_1 - s_2}\frac{\sigma_0}{2}\left(\sqrt{z_2^2 - a^2} - z_2\right) \tag{6b}$$

where a is the half crack length. Substitution of eqn (6) into eqn (2) leads to the following expression for v_2:

$$v_2 = 2Re[q_1\phi_2(z_1) + q_2\psi_2(z_2)] \tag{7}$$

For the case shown in Fig. 2c, the sheet contains no crack and is subjected to a single concentrated force F located at point (x_0, y_0), the Kolosov–Muskhelishvili complex stress functions (Lekhnitskii, 1968) are given by:

$$\phi_3(z_1) = C_{12}\frac{F}{t}\log(z_1 - z_{10}) \tag{8a}$$

$$\psi_3(z_2) = C_{22}\frac{F}{t}\log(z_2 - z_{20}) \tag{8b}$$

in which

$$z_{m0} = x_0 + s_m y_0 \quad (m = 1, 2) \tag{9}$$

$$C_{12} = \frac{1}{2\pi i}\frac{s_2\bar{s}_2 + \bar{s}_1 s_2 + \bar{s}_1\bar{s}_2 + v_x}{(s_1 - s_2)(s_1 - \bar{s}_1)(1 - \bar{s}_2/s_1)} \tag{10a}$$

$$C_{22} = \frac{1}{2\pi i}\frac{s_1\bar{s}_1 + \bar{s}_2 s_1 + \bar{s}_2\bar{s}_1 + v_x}{(s_2 - s_1)(s_2 - \bar{s}_2)(1 - \bar{s}_1/s_2)} \tag{10b}$$

where t is the thickness of the sheet, $i = \sqrt{-1}$ and $\bar{s}_m$ are the complex conjugates of s_m for $m = 1, 2$. Note that eqn (8) contains a singularity at the point (x_0, y_0) and cannot be used in its present form to calculate the displacement at this point. This problem is eliminated by distributing the concentrated force, F, uniformly over the fastener diameter, d. Using eqn (8) to obtain the stress functions of a distributed load and integrating the effect over the fastener diameter will yield the following equation free from the singularity at the load point:

$$\phi_3(z_1) = C_{12}\frac{F}{td}\big[(z_1 - z_{10} + d/2)\ \log(z_1 - z_{10} + d/2) - (z_1 - z_{10} - d/2)\ \log(z_1 - z_{10} - d/2)\big] \tag{11a}$$

$$\psi_3(z_2) = C_{22}\frac{F}{td}\big[(z_2 - z_{20} + d/2)\ \log(z_2 - z_{20} + d/2) - (z_2 - z_{20} - d/2)\ \log(z_2 - z_{20} - d/2)\big] \tag{11b}$$

The displacement v_3 of the uncracked sheet resulting from the fastener force F is obtained by substituting eqn (8) (or eqn (11) for the load point) into eqn (2):

$$v_3 = 2Re\big[q_1\phi_3(z_1) + q_2\psi_3(z_2)\big] \tag{12}$$

and the corresponding stress distribution anywhere in the sheet can be determined as follows:

$$\sigma_x(x, y) = 2Re\Big[s_1^2\phi_3'(z_1) + s_2^2\psi_3'(z_2)\Big] \tag{13a}$$

$$\sigma_y(x, y) = 2Re\big[\phi_3'(z_1) + \psi_3'(z_2)\big] \tag{13b}$$

$$\tau_{xy}(x, y) = -2Re\big[s_1\phi_3'(z_1) + s_2\psi_3'(z_2)\big] \tag{13c}$$

where $(\,)'$ signifies differentiation of a function with respect to its argument. On the real axis $z = x$, the stresses σ_y and τ_{xy} take on the forms

$$\sigma_y(x, 0) = 2Re\left[\left(\frac{C_{12}}{x - z_{10}} + \frac{C_{22}}{x - z_{20}}\right)\frac{F}{t}\right] \tag{14a}$$

$$\tau_{xy}(x, 0) = -2Re\left[\left(\frac{s_1 C_{12}}{x - z_{10}} + \frac{s_2 C_{22}}{x - z_{20}}\right)\frac{F}{t}\right] \tag{14b}$$

Applying these stresses to the surface of the crack shown in Fig. 2d, the following complex stress functions for the displacement v_4 can be obtained by integrating eqn (4.27) in Sih and Liebowitz (1968):

$$\begin{aligned}\phi_4(z_1) = -\frac{F}{2(s_2 - s_1)t}\Big[&s_2\Big(C_{12}g(z_1, z_{10}) + \bar{C}_{12}g(z_1, \bar{z}_{10}) + C_{22}g(z_1, z_{20}) + \bar{C}_{22}g(z_1, \bar{z}_{20})\Big)\\ &- \Big(s_1 C_{12}g(z_1, z_{10}) + \bar{s}_1\bar{C}_{12}g(z_1, \bar{z}_{10}) + s_2 C_{22}g(z_1, z_{20}) + \bar{s}_2\bar{C}_{22}g(z_1, \bar{z}_{20})\Big)\Big]\end{aligned} \tag{15a}$$

$$\psi_4(z_2) = -\frac{F}{2(s_1 - s_2)t}\Big[s_1\Big(C_{12}g(z_2, z_{10}) + \bar{C}_{12}g(z_2, \bar{z}_{10}) + C_{22}g(z_2, z_{20}) + \bar{C}_{22}g(z_2, \bar{z}_{20})\Big) - \Big(s_1 C_{12}g(z_2, z_{10}) + \bar{s}_1\bar{C}_{12}g(z_2, \bar{z}_{10}) + s_2 C_{22}g(z_2, z_{20}) + \bar{s}_2\bar{C}_{22}g(z_2, \bar{z}_{20})\Big)\Big] \quad (15b)$$

where

$$g(z, z_0) = \log\left(z \cdot z_0 - a^2 + \sqrt{z^2 - a^2}\sqrt{z_0^2 - a^2}\right) - \log\left(z + \sqrt{z^2 - a^2}\right) \quad (16)$$

Substitution of eqn (15) into eqn (2) results in the following equation for the displacement v_4:

$$v_4 = 2Re\big[q_1\phi_4(z_1) + q_2\psi_4(z_2)\big] \quad (17)$$

Finally, the total displacement of the cracked orthotropic sheet due to the remote tensile stress and fastener reaction forces can be expressed as:

$$v_t = v_1 + v_2 + \sum_{i=1}^{j}\big[v_3(F_i) + v_4(F_i)\big] \quad (18)$$

where j is the number of fasteners and F_i is the reaction force at the i-th fastener.

2.2. Fastener displacements

The i-th fastener displacement due to the fastener reaction force F_i is given as follows:

$$v_{fi} = F_i * f(v) \quad (19)$$

where v is the shear displacement of the fastener; f denotes the fastener flexibility and can be a function of fastener shear displacement. The empirical expressions of f at the initial linear elastic stage for aluminum and steel rivets have been determined from tests (Swift, 1984).

2.3. Stiffener displacements

The displacements for intact and broken stiffeners are analyzed using a similar approach reported by Poe (1973) and Swift (1984). The intact stiffener displacements v_{gi} due to the applied stress σ_0 of the sheet are given by:

$$v_{gi} = \frac{F_e}{E_s}\sum_{j=1}^{i}\frac{y_j - y_{j-1}}{A_j} \quad (20)$$

where E_s is the Young's modulus of the stiffener; A is the cross-sectional area of stiffener between the fasteners; y is the fastener coordinates from the crack center line; and the force, F_e, applied at the end of stiffener is obtained from the following equation by assuming that the displacement of the sheet is equal to the stiffener displacement at the N-th active fastener:

$$\frac{\sigma_0}{E_y}y_N = \frac{F_e}{E_s}\sum_{i=1}^{N}\frac{y_i - y_{i-1}}{A_i} \quad (21)$$

N is the number of active fasteners per stiffener. The intact stiffener displacements v_{di} due to direct fastener forces F are given by:

$$v_{\mathrm{di}} = \frac{1}{E_{\mathrm{s}}} \sum_{j=1}^{i} \frac{y_i - y_{j-1}}{A_j} \sum_{k=j}^{N} F_k \tag{22}$$

Similarly, the broken stiffener displacements due to the fastener forces are defined from the N-th active fastener and are given by:

$$v_{\mathrm{di}} = \frac{1}{E_{\mathrm{s}}} \sum_{j=i+1}^{N} \frac{y_j + y_{j-1}}{A_j} \sum_{k=1}^{j-1} F_k \tag{23}$$

Note that the above equations are valid until the stiffener stress reaches the yield strength of the stiffener. If the applied stresses are not too high, small scale stiffener yielding does not drastically effect the results obtained from the elastic analysis (Yeh, 1993). However, if this is not the case then a nonlinear analysis is usually required.

2.4. Displacement compatibility

In the previous sections, the displacements of the cracked orthotropic sheet, fasteners, and stiffeners are presented. Thus, a system of simultaneous equations with unknown fastener forces is set up by making a series of displacements in the cracked sheet compatible with those of the stiffeners and fasteners at the junction line of fastener arrays. The size of the compatibility matrix is equal to the total number of active fasteners. Then, the compatibility matrix is inverted and unknown fastener forces are solved. A detailed description of the displacement compatibility method can be found in Swift (1984).

The computer program developed by Yeh (1993) earlier for the elastic analysis, is extensively modified to handle two nonlinear behaviors of the riveted stiffened panel. They are the nonlinear load-displacement behavior of the fastener and the elastic-plastic behavior of the stiffener. A direct iteration approach using the trial and error process, is chosen to solve the nonlinear problem (Zienkiewicz, 1977). A linear elastic solution is generated initially based on the initial slopes of the fastener load-deflection and stiffener stress-strain curves. These slopes are then modified according to the resulting fastener force and the corresponding stiffener stress between adjacent rivets. A new solution is obtained based on these new slopes. The crack-tip stress intensity factor obtained from the first solution is compared to that obtained from the second solution. If the difference is greater than a set number, which can be adjusted, then the procedure is automatically repeated. The iterative process continues automatically until the stress intensity factor between iterations drops below the specified value, and at this time a final solution at the given crack size and input gross stress is output. The program is set to handle different applied stress levels and different crack sizes in a single run.

3. Fracture mechanics parameters at the crack tip

In examining the stability of cracks, it is customary to determine the stress intensity factor and energy release rate at the crack tip. These two fracture mechanics parameters may be obtained from the stress and displacement fields near the crack tip as follows (Irwin, 1957):

$$K_1 = \lim_{r \to 0} \sqrt{2\pi r}\, \sigma_y(r, 0) \tag{24}$$

$$G_1 = \lim_{c\to 0}\frac{1}{c}\int_0^c \sigma_y(r,0)\, v(c-r,\pi)\, \mathrm{d}r \tag{25}$$

where c is the length of virtual crack extension. The stress, σ_y, and the displacement, v, are expressed in terms of polar coordinates r and θ (see Fig. 1). Therefore, in order to determine the fracture mechanics parameters, we need to transform the Cartesian coordinates used in the previous section to polar coordinates. This can easily be done by letting

$$x = a + r\cos(\theta) \quad y = r\sin(\theta) \tag{26}$$

Since only the asymptotic stress and displacement distributions around the crack tip are needed in eqns (24) and (25), we can further assume that r is small in comparison with the half crack length a. Based on the above arguments, σ_y and v can be obtained in terms of the remote tensile stress and the active fastener forces:

$$\sigma_y(r,0) = \frac{1}{\sqrt{2r}}H \tag{27}$$

$$v(r,\pi) = \sqrt{2r}H \;\; Re\left(\frac{q_1 s_2 - q_2 s_1}{s_2 - s_1} i\right) \tag{28}$$

in which

$$H = \sigma_0\sqrt{a} - \sum_{j=1}^{M}\frac{F_j}{t\sqrt{a}} 2Re\left[C_{12}J(z_{1j}) + C_{22}J(z_{2j})\right] \tag{29}$$

$$J(z) = 1 - \frac{\sqrt{z+a}}{\sqrt{z-a}} \tag{30}$$

where M is the total number of active fasteners. Substitution of eqns (27) and (28) into eqns (24) and (25) yields the fracture mechanics parameters K_I and G_I of the stiffened sheet due to the remote tensile stress and the fastener forces (Yeh, 1988, 1989).

$$K_\mathrm{I} = \sqrt{\pi}H \tag{31}$$

$$G_\mathrm{I} = \frac{\pi}{2}H^2 Re\left(\frac{q_1 s_2 - q_2 s_1}{s_2 - s_1} i\right) \tag{32}$$

A limiting case of unstiffened panel is considered by assuming all fastener forces equal to zero in eqns (31) and (32). The following expressions for the stress intensity factor and energy release rate of a cracked sheet subjected to an uniform applied stress are obtained:

$$K_\mathrm{I}^* = \sigma_0\sqrt{\pi a} \tag{33}$$

$$G_\mathrm{I}^* = \sigma_0^2 \pi a \frac{1}{2} Re\left(\frac{q_1 s_2 - q_2 s_1}{s_2 - s_1} i\right) \tag{34}$$

which are identical to the solution given by Sih and Liebowitz (1968). It can also be shown that $(K_I/K_I^*)^2 = G_1/G_1^*$

4. Numerical results and discussion

To demonstrate the applicability and accuracy of the present approach, three types of problems shown in Fig. 3 are studied using both the present analytical method and the finite element method. They are: Case (a) one-bay crack, Case (b) two-bay crack with center stiffener intact and Case (c) two-bay crack with center stiffener broken. The study is conducted using one typical fuselage configuration with sheet thickness 1 mm, stiffeners spaced 250 mm apart with cross-sectional area 150 mm^2, and fastener spacing 25 mm with fastener diameter 5 mm. For the purpose of this exercise, the sheet is chosen to be an orthotropic laminate and the stiffeners are chosen to be 7075-T6 aluminum alloy. Material properties are listed in Table 1

Although the effects of the bending flexibilities of the sheet and stiffeners are already incorporated into the computer program, these effects are not included in the present calculations. Moreover, the friction forces between the sheet and stiffeners are neglected and the loss of stiffener area due to the fastener holes is ignored in the analysis.

Since the effect of the fasteners far away from the crack is negligibly small, computing time can be minimized by reducing the number of fasteners used to a reasonable level while still maintaining the desired degree of accuracy. The sensitivity of the number of fasteners considered has been studied earlier. Poe (1973) and Swift (1984) have found 5 and 15 fasteners to be appropriate for isotropic sheets with intact and broken stiffeners, respectively. Similar conclusions were also obtained for stiffened orthotropic sheet (Yeh, 1993). Therefore, 15 fasteners are used in this study in order to obtain a converged solution consistently.

The effects of the nonlinear shear deformation of the fastener are studied first. The corresponding

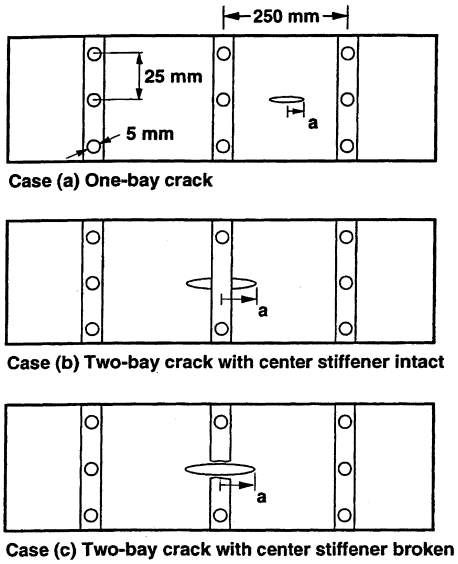

Fig. 3. Cases studied to verify model.

Table 1
Material properties used in the study

Orthotropic laminated skin
$E_y = 68{,}000$ MPa
$E_x = 48{,}000$ MPa
$G_{xy} = 17{,}000$ MPa
$\nu_y = 0.33$
$\nu_x = 0.23$
Aluminum 7075-T6
$E = 71{,}000$ MPa
$\nu = 0.33$
$\sigma_y = 505$ Mpa

force due to the nonlinear shear deformation is applied at all the fastener locations. A piecewise linear load-displacement model obtained from Swift (1984) is used here and the data are listed in Table 2. From the displacement compatibility analysis, the resulting normalized stress intensity factors (K_I/K_I^*) as a function of half crack length, a, are obtained and plotted in Figs. 4–6 for Cases (a)–(c) shown in Fig. 3, respectively. Note that K_I^* is defined in eqn (33). For comparison, the resulting normalized stress intensity factors for perfect rigid fasteners are also plotted in the figures (denoted as Rigid). It can be seen that in some cases the value of stress intensity factors is increased due to the effects of the nonlinear shear deformation of fastener.

Finite element analyses using ABAQUS are also conducted for these cases. Due to symmetry, only a quarter of the sheet is divided into four-node plane stress elements and the stiffeners are discretized by two-node truss elements. The truss elements are connected to the sheet by nonlinear spring elements. The finite element mesh for Case (a) consists of 2646 nodes, 2542 plane stress, 16 truss and 15 spring elements. Similar meshes utilizing 32 truss and 30 spring elements are used for Cases (b) and (c). The finite element results are also shown in Figs. 4–6 for comparison. It can be seen that good agreement is obtained for the cases studied.

The effects of the plastic deformation of the stiffener are studied next. A elastic-perfectly plastic stress-strain model is used and the yield strength of 7075-T6 aluminum alloy is set to be 505 MPa. Two types of stiffeners are considered in this study: (A) stiffeners having a constant cross-sectional area of 150 mm^2 and (B) stiffeners where the area inside the first rivet is reduced from 150 mm^2 to 100 mm^2. The latter type is used to simulate a frame detail where the frame is cut to accommodate continuous stringers passing through the frames. From the displacement compatibility analysis, the resulting normalized stress intensity factors as a function of the half crack length are obtained and plotted in Figs. 7–9 for Cases (a)–(c) shown in Fig. 3, respectively. For comparison, the resulting normalized stress intensity

Table 2
Piecewise linear model for fastener shear deformation (Swift, 1984)

Force (N)	Displacement (mm)
0	0
3252	0.0737
4811	0.2591
5568	0.7264

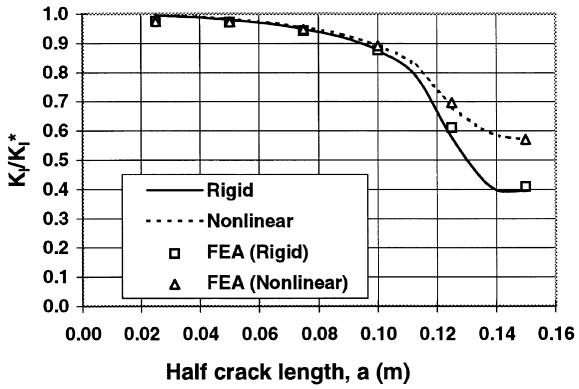

Fig. 4. Normalized stress intensity factor for an orthotropic cracked stiffened panel with nonlinear shear deformation of the fastener (one-bay crack case).

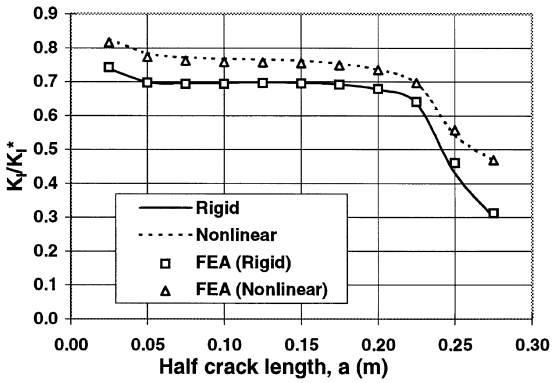

Fig. 5. Normalized stress intensity factor for an orthotropic cracked stiffened panel with nonlinear shear deformation of the fastener (two-bay crack case with central stiffener intact).

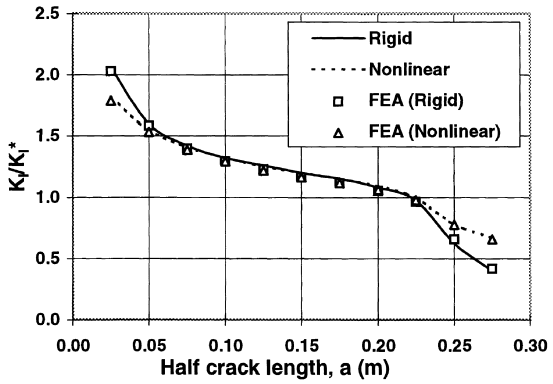

Fig. 6. Normalized stress intensity factor for an orthotropic cracked stiffened panel with nonlinear shear deformation of the fastener (two-bay crack case with central stiffener broken).

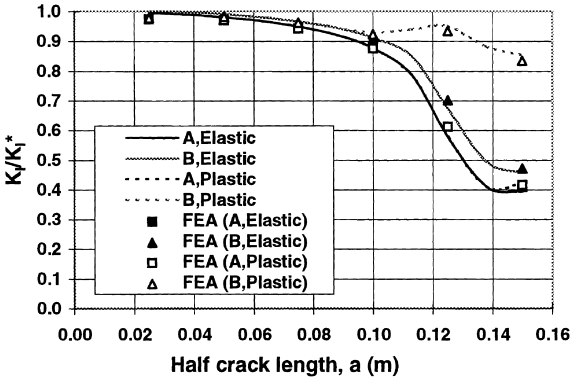

Fig. 7. Normalized stress intensity factor for an orthotropic cracked stiffened panel with plastic deformation of the stiffener (one-bay crack case).

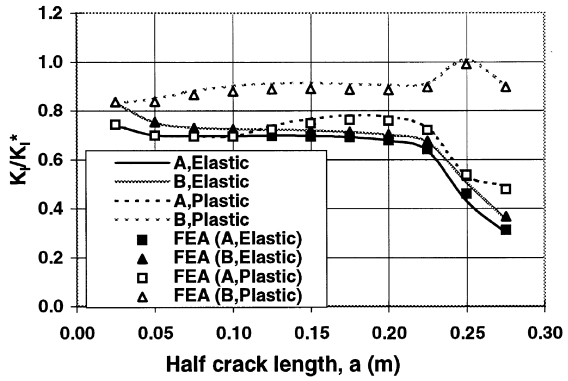

Fig. 8. Normalized stress intensity factor for an orthotropic cracked stiffened panel with plastic deformation of the stiffener (two-bay crack case with central stiffener intact).

factors for linear elastic stiffeners are also plotted in the figures (denoted as Elastic). It can be seen that in some cases the value of stress intensity factors is significantly increased due to the effects of the plastic deformation and the area reduction of the stiffener. The finite element results are also shown in Figs. 7–9 for comparison. Again, good agreement is obtained for the cases studied.

Finally, the combined effects of the nonlinear shear deformation of the fastener and the elastic-plastic deformation of the stiffener are studied. The resulting normalized stress intensity factors for both stiffener types (A and B) are obtained and plotted in Figs. 10–12 for Cases (a)–(c) shown in Fig. 3, respectively. It is not a surprise to see that in some cases the stress intensity factors of stiffener type B are much higher than stiffener type A. It should be mentioned that for stiffener type A, the stress intensity factors are dominated by the fastener nonlinear shear deformation, and for stiffener type B, the stress intensity factors are controlled by the stiffener plastic deformation. The finite element results are also shown in Figs. 10–12 for comparison. It can be seen that good agreement is obtained for the cases studied.

As mentioned in Section 2.4 for nonlinear analyses, the iterative process continues until the difference of stress intensity factor between iterations drops below a specified value, e. In other words, the analysis stops when $|1 - K_{n-1}/K_n| < e$. The value of e was set to be 0.0001 in this study in order to obtain a

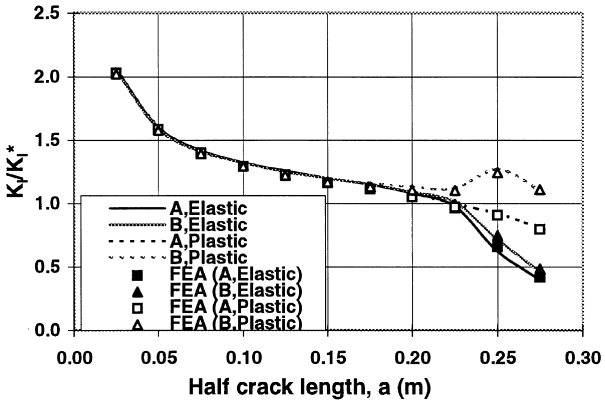

Fig. 9. Normalized stress intensity factor for an orthotropic cracked stiffened panel with plastic deformation of the stiffener (two-bay crack case with central stiffener broken).

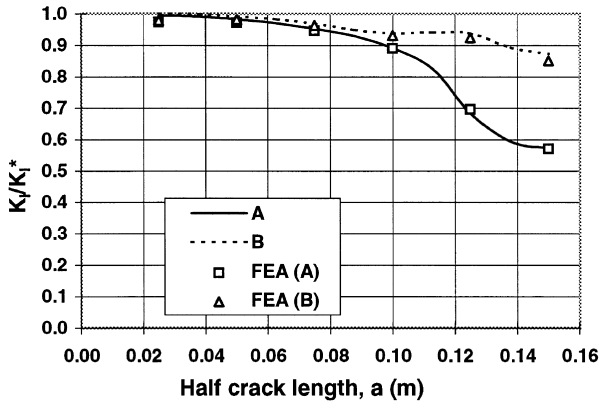

Fig. 10. Normalized stress intensity factor for an orthotropic cracked stiffened panel with fastener nonlinear shear and stiffener plastic deformations (one-bay crack case).

converged solution. Note that for all the cases studied in the paper, a converged solution was always obtained and the maximum number of iteration required was 41.

The agreement between the analytical and finite element results for all the cases presented provides the validity of the present closed form solution of cracked orthotropic sheets for the displacement compatibility analysis with the effects of the fastener nonlinear shear deformation and the stiffener plastic deformation. Note that the analytical method requires much shorter computer run time and fewer input data than the finite element analysis, so parametric studies for damage tolerance assessment can be made more easily and at a lower cost.

5. Conclusions

A closed form solution for cracked orthotropic sheets with riveted stiffeners is presented. The effects of the fastener nonlinear shear deformation, the stiffener plastic deformation, and the stiffener cutouts

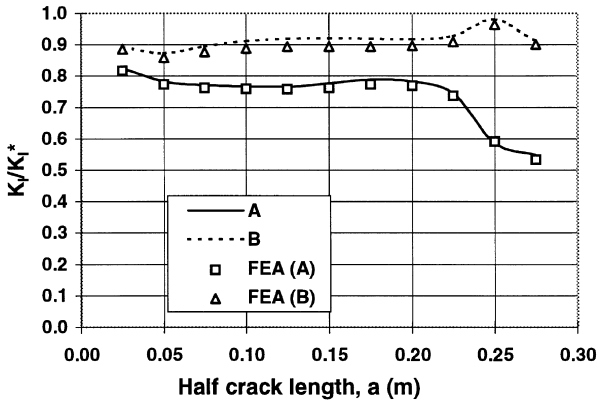

Fig. 11. Normalized stress intensity factor for an orthotropic cracked stiffened panel with fastener nonlinear shear and stiffener plastic deformations (two-bay crack case with central stiffener intact).

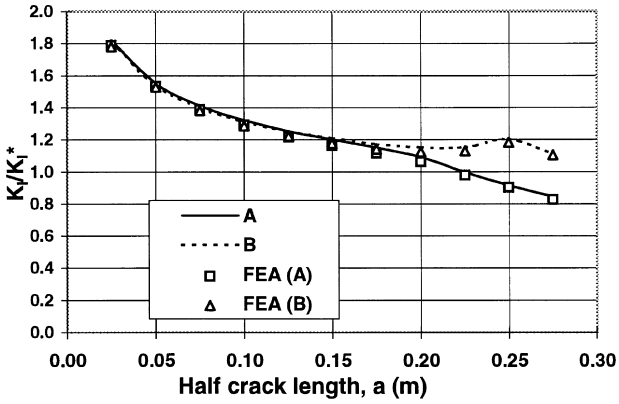

Fig. 12. Normalized stress intensity factor for an orthotropic cracked stiffened panel with fastener nonlinear shear and stiffener plastic deformations (two-bay crack case with central stiffener broken).

are included in the analysis. The stiffener cutouts are used to simulate a frame detail where the frame is cut to accommodate continuous stringers passing through the frames. Stress intensity factors and energy release rates are determined based on compatibility of displacements among the sheet, fasteners and stiffeners. Three example problems, one-bay crack and two-bay crack with center stiffener either intact or broken, are solved and the results are verified by finite element analysis. The present method is ideal for parametric studies of basic structural configurations because of its relatively low computer costs.

References

Irwin, G.R., 1957. Analysis of stress and strains near the end of a crack traversing a plate. J. Appl. Mech 24, 361–364.

Lekhnitskii, S.G., 1968. Anisotropic Plates. Gordon and Breach, New York.

Nishimura, T., 1991. Stress intensity factors for a cracked stiffened sheet with cracked stiffeners. Journal of Engineering Materials and Technology 113, 119–124.

Poe Jr, C.C., 1973. The effect of broken stringers on the stress intensity factor for a uniformly stiffened sheet containing a crack. NASA TM X-71947. NASA Langley Research Center, Hampton, VA.

Romualdi, J.P., Frasier, J.T., Irwin, G.R., 1957. Crack-extension-force near a riveted stiffener. NRL Report 4956.
Swift, T., 1984. Fracture analysis of stiffened structure. In: Chang, J.B., Rudd, J.L. (Eds.), Damage Tolerance of Metallic Structures: analysis methods and application, ASTM STP, 842, pp. 69–107.
Sih, G.C., Liebowitz, H., 1968. Mathematical theories of brittle fracture. In: Liebowitz, H. (Ed.), Fracture: An Advanced Treatise. Academic Press, New York, pp. 108–131.
Yeh, J.R., 1988. Fracture mechanics of delamination in ARALL laminates. Journal of Engineering Fracture Mechanics 30, 827–837.
Yeh, J.R., 1989. The mechanics of multiple transverse cracking in composite laminates. Int. J. Solids Structures 25, 1445–1455.
Yeh, J.R., 1993. Fracture analysis of a stiffened orthotropic sheet. Journal of Engineering Fracture Mechanics 46, 857–866.
Yeh, J.R., 1995. Fatigue crack growth in fiber-metal laminates. Int. J. Solids Structures 32, 2063–2075.
Zienkiewicz, O.C., 1977. The Finite Element Method, 3rd ed. McGraw-Hill.